

## Research Article

# Supramolecular Enhancement of BODIPY Singlet Oxygen Generation Using Bile Salt Micelles

Sharvani Regmi<sup>1#</sup>; Ashley Maharjan<sup>1#</sup>; Vijayakumar Ramalingam<sup>2</sup>; Elamparuthi Ramasamy<sup>3</sup>; Mahesh Pattabiraman<sup>1\*</sup>

<sup>1</sup>University of Nebraska Kearney, Kearney, NE – 68845, USA

<sup>2</sup>Department of Biology and Chemistry, SUNY Polytechnic Institute, Utica, NY 13502, USA

<sup>3</sup>Department of Chemistry and Biochemistry, The University of Texas at Arlington, Arlington, TX 76019, USA

\*Corresponding author: Mahesh Pattabiraman

University of Nebraska Kearney, Kearney, NE – 68845, USA.

Email: pattabiram2@unk.edu

#These authors have contributed equally to this article.

Received: October 04, 2023

Accepted: October 30, 2023

Published: November 06, 2023

## Introduction

Singlet Oxygen (*SO*) refers to the electronically excited spin isomer of ambient triplet oxygen [1,2]. As a highly reactive excited state intermediate generated in atmospheric and biological systems, it possesses significance in many processes such as planetary chemistry, photosynthesis [3,4], oxidative stress [5], immune response [6], and cellular signaling [7]. Singlet Oxygen Generation (*SOG*), its reactivity [8-10], and excited state dynamics are the subject of much research interest in medical technologies leading to the development of therapeutic modality known as photodynamic therapy [11,12], which is implemented in treatment of certain types of cancer, skin conditions [13-15], macular degeneration [16], acne [17], and psoriasis [18]. The importance of this species is demonstrated by the sheer volume of published works that document its reactivity, excited state dynamics, and behavior in different media and versatility in its applications. Thus, there is significant interest in designing new dyes and methodologies to generate *SO* for afore-mentioned applications.

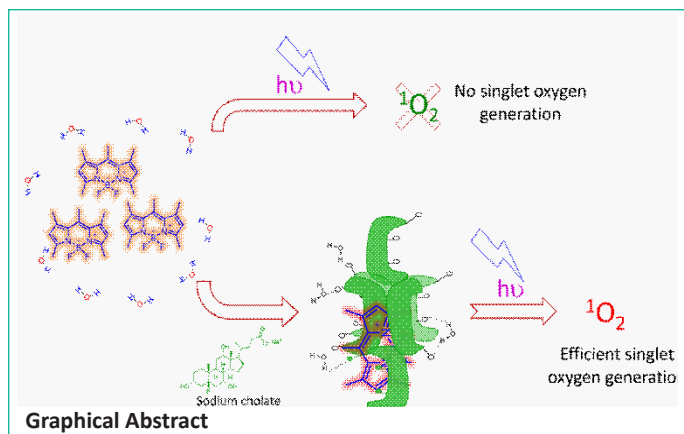
## Abstract

Singlet Oxygen (*SO*) generation is the core chemical process of many medical and industrial applications. Designing efficient *SO*-Generating (*SOG*) agents is a major research focus for its utility in photodynamic therapy, wastewater treatment, material science, and organic synthesis. Photosensitization of ambient oxygen using organic dyes is an efficient approach to generating *SO*, though their efficiency is often severely hampered due to aggregation-induced deactivation. In this manuscript, we present the utility of bile salt micelle as supramolecular host for promoting *SOG* in aqueous media for a BODIPY dye, which was otherwise highly inactive. The *SOG* efficiency in test media was probed by monitoring the oxidation of 1,5-Dihydroxy Naphthalene (DHN) to corresponding quinone (juglone) through spectroscopic and chromatographic methods. In this study, we investigated the use of bile salt micelles as a supramolecular platform for enhancing the *SOG* efficiency of a BODIPY dye in aqueous media through complexation. Our results show that sodium cholate micelles can solubilize the hydrophobic dye and enhance its ability to generate singlet oxygen, while traditionally used macrocyclic hosts such as  $\beta$ - and  $\gamma$ -cyclodextrin complexation was found to be far less efficient. Computational modeling revealed that the bile salt micelles form an aggregated complex structure with the dye, leading to improved supramolecular interactions and photophysical properties. This work demonstrates the potential of bile salt micelles as a natural and safe platform for enhancing the activity of nonpolar dyes for PDT applications.

**Keywords:** Singlet oxygen; Bile salt micelle; Sodium cholate; Cyclodextrins; Supramolecular chemistry; Photodynamic therapy; Photochemistry.

There is vast literature of designed photosensitizers with competitive *SOG* efficiencies, relatively little effort is dedicated towards non-covalently finetuning the dyes to improve activity. In this context there have been supramolecular photochemistry efforts that have utilized weak interactions, such as through host-guest chemistry, to increase *SOG* [19-21]. Herein we report the use of bile salt micelles in enabling a BODIPY dye to efficiently generate singlet oxygen in aqueous medium through complexation. Our efforts, as outlined in this manuscript, leads to understanding of the supramolecular interactions that lead to enhancement of activity, and serves as a demonstration of a natural and benign surfactant as promising and safe platform for solubilizing a simple and otherwise inactive dye for generating *SO* without covalent modification.

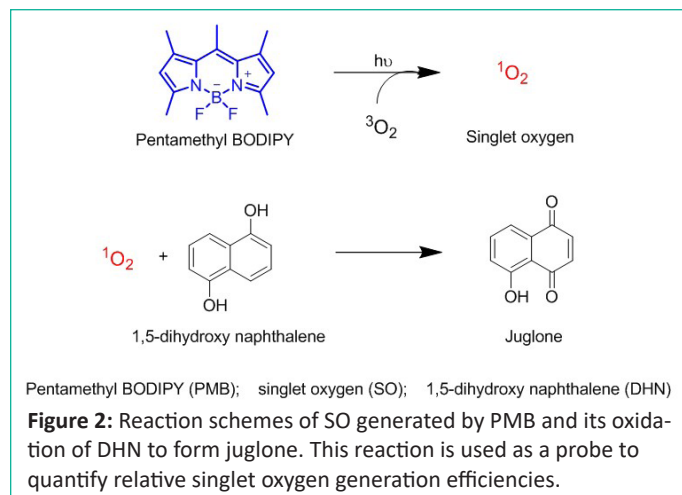
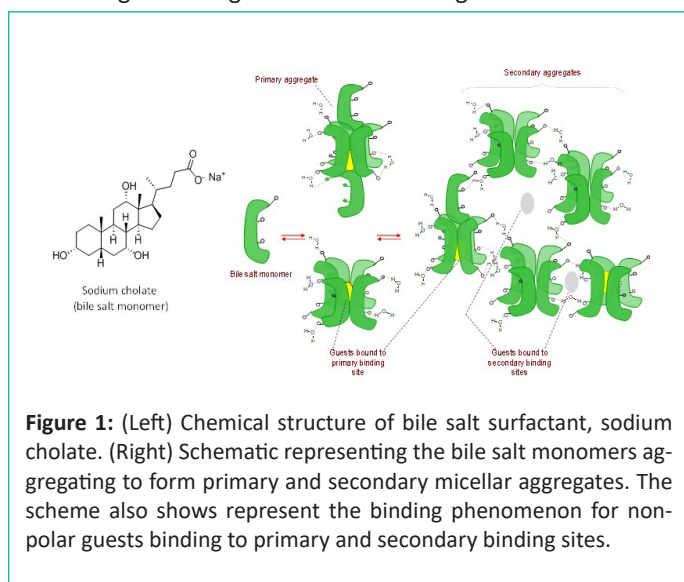
Though there are notable works and a broad literature of supramolecular *SOG* in micelles, there has been no such report for the same in bile salt micelle. Thus, this work is expected to



intrigue researchers in relevant fields to explore bile salt micelles as potential drug delivery agents in the context of PDT and otherwise.

### Bile Salt Micelles

In this study we employed two supramolecular hosts systems – sodium cholate micelles (a bile salt) [22] and cyclodextrins – to manipulate the SOG efficiency of a BODIPY dye, which was remarkably hampered in water, compared to methanol, due to aggregation-induced non-radiative relaxation. Cyclodextrins, cucurbiturils, dendrimers, and other macromolecular hosts, and traditional surfactants are well-known macromolecular systems that have been used to disaggregate dyes to achieve photophysical manipulation [19]. However, bile-salt micelles (Figure 1) have not been used in this context despite their practically useable low toxicity as drug delivery agent, unique host-guest characteristics, and demonstrated ability to solubilize drug molecules [23–25]. They are a relatively less known supramolecular system and have not been used in a similar context to the best of our knowledge. They are physiologically produced in mammals and play an important role in fat digestion [26,27]. These steroidal compounds, unlike synthetic surfactants, display highly unusual aggregation behavior. For one they have traversal spatial distribution of polar and non-polar groups leading to a small aggregation number (3 to 7), standing/upright aggregate structure, and low CMC [28]. They also undergo stepwise micelle formation wherein at very low concentrations three to five monomers self-assemble to form primary aggregates, and as concentration increases, the primary aggregates further assemble in weakly held networks to form secondary aggregates. Thus, the primary and secondary aggregates afford two different binding sites for guests as shown in Figure 2.



### BODIPY Dyes

BODIPY (boron-dipyrromethene) dyes have emerged as promising photosensitizers for Singlet Oxygen Generation (SOG) due to their strong absorption in the visible region and high overall singlet oxygen quantum yields [29]. BODIPY-based photosensitizers have shown great potential in Photodynamic Therapy (PDT) for the treatment of cancer and other diseases, offering improved selectivity and reduced side effects compared to traditional cancer therapies. However, BODIPY-based photosensitizers can be limited by their relatively short singlet oxygen lifetime, which may require higher concentrations and longer treatment times to achieve therapeutic efficacy. The solubility of BODIPY-based photosensitizers can also be a limitation, as some derivatives may exhibit poor solubility in aqueous solutions, which can affect their bioavailability and hinder their use in photodynamic therapy.

BODIPY dyes are pursued for their versatile photophysics as they possess strong molar absorptivity ( $10^4 \text{ M}^{-1} \text{ cm}^{-1}$ ) and exhibit high fluorescent quantum yields ( $\Phi$  ca. 0.5–0.8) due to which they are highly sought after as imaging agents in biomedicine and diagnostics. They also possess favorable properties that contribute to the tunability of their Intersystem Crossing (ISC) efficiencies, to populate long-lived Triplet excited states ( $T_1$ ). The combination of heavy atom substitution and structural rigidity in BODIPY dyes enhances their spin-orbit coupling, facilitating rapid ISC from the initially excited Singlet State ( $S_1$ ) to the Triplet state ( $T_1$ ). This efficient ISC process enables BODIPY dyes to engage in various photophysical phenomena and broaden their range of applications in fields such as triplet state chemistry, energy transfer, and singlet oxygen generation.

In this communication, we report our effort in using host-guest chemistry to render a highly water-insoluble BODIPY dye (1,3,5,7-tetramethyl BODIPY, PMB) soluble in aqueous medium and improve its ability to generate singlet oxygen. PMB was chosen for its notably low solubility in water, simplicity and synthetic accessibility, low molecular weight, and compact structure to be easily accommodated within macrocyclic hosts. Our studies feature our observation of two different supramolecular hosts and how they influence SOG efficiency of BODIPY with curiously contrasting outcomes.

SOG efficiency was monitored through the spectroscopic and chromatographic monitoring of SO oxidation of 1,5-DHN to its quinone product, juglone. This reaction was chosen as their absorption profiles do not overlap significantly allowing for monitoring of spectral changes to represent SOG.

## Experimental Section

### Materials and Methods

Substances were purchased from commercial sources: sodium cholate hydrate (206986-87-0, Aldrich); pentamethyl BODIPY (CAS 121207-31-6, Millipore Sigma); 1,5-dihydroxy naphthalene (CAS 83-56-7, Fisher Sci.);  $\beta$ -cyclodextrin hydrate (CAS 7585-39-9, Wako Chemicals);  $\gamma$ -Cyclodextrin (CAS 17465-86-0, Wako Chemicals). Solvents are of ACS reagent grade quality and were purchased from commercial sources. All aqueous solutions were prepared using deionized water with a resistivity of at least 18.0 M $\Omega$ -cm obtained from a Milli-Q water purification system (MilliporeSigma).

**Preparation of UV-Vis solutions** was achieved by dispensing aliquots of compounds from stock solutions prepared in methanol. Typical procedure involved preparing stock solutions of the respective compounds in methanol in a 15 mL standard flask; typical concentrations of PMB were around 5 mM (~20 mg in 15 mL), and that for DHN were around 10 mM (~25 mg in 15 mL). Then, the stock solutions were diluted by dispensing 50 mL of PMB and 25 mL of DHN into methanol or water solutions to achieve a total volume of 5 mL in a 20 mL Pyrex test tube. Based on the original stock solutions, the final concentrations of resulting solutions were close to  $5 \times 10^{-5}$  M for PMB and  $5.7 \times 10^{-5}$  M for DHN. From this 3 mL of the solution was transferred into a cuvette fitted with a septum and subject to oxygen purging and exposure to white light. While methanol solution was completely clear and homogeneous, the aqueous solutions showed a slight change in visible color of PMB. However, there was no significant turbidity in the solutions due to low concentration. Sodium cholate and cyclodextrin complex solutions were prepared by adding the hosts to the respective aqueous solutions and stirring them for two hours before subjecting them to photochemical step. Quartz cuvettes were used for the experiments and spectra were recorded in a dual beam Shimadzu UV-1900-i UV-Vis spectrophotometer.

**Oxygen Purging Step** was performed with a commercial home oxygen generator equipment (Osito® portable oxygen concentrator), which delivered a 85% to 90% gas mixture at a constant flow rate of 150 mL/min; the oxygen percentage was verified using an oxygen sensor purchased from Vernier Scientific. The Pyrex tubes with solutions were secured with a rubber septum and an outlet tube from oxygen meter was fitted with a purging needle that bubbled the gas into the solution. A hypodermic short stem needle was plunged into the rubber septum for pressure release.

**Irradiation Conditions** The samples containing DHN and PMB that was purged with oxygen was subject to photochemical excitation using a commercially available 150 Watt LED white light source at a color temperature of 5000 K.

**GC-MS analysis** was performed on an Agilent 7820 A equipment. Methanol and water samples were injected as such. The pure methanol GC-MS experiment was performed at concentration of  $4.33 \times 10^{-4}$  M for PMB and  $5.20 \times 10^{-4}$  M for DHN. Sodium cholate samples were prepared at  $4.33 \times 10^{-4}$  M for PMB,  $5.20 \times 10^{-4}$  M for DHN, and 11 mM for NaCh at a total volume of 5 mL. For GC-MS analysis, the solutions were first diluted to thrice the volume and stirred with 5 mL of ethyl acetate for two hours. The resulting organic layer was injected into the GC-MS as such.

**Computational chemistry** studies were performed using Spartan '20 software installed in a windows desktop with AMD

A10-5800 K with 10 cores operating at a frequency of 3.8 Gz, and 60 GB of physical RAM. Sodium cholate and PMB structures were generated using Chem 3D and transferred into Spartan as a pdb file. Structure optimizations were performed in SE PM3 level first, and then final structure was further used to compute at HF STO-3G level.

### Results and Discussion

We employed the oxidative reactivity of SO with DHN (1,5-dihydroxy naphthalene) as a probe for relative quantification of SOG efficiencies (Figure 2). DHN is known to be oxidized by SO to its corresponding naphthoquinone (juglone) when generated in presence of PS in the same medium. In order to understand the baseline SOG efficiency in homogeneous medium, we studied the time-dependent generation rate in methanol.

A solution mixture containing  $4.33 \times 10^{-4}$  M PMB and  $5.20 \times 10^{-4}$  M DHN prepared in methanol was purged with oxygen and exposed to white light and sample collected periodically with intervals ranging from 15 mins to 20 mins for approximately one hour and the reaction mixture was monitored in a GC-MS (Supporting Information). As expected, initially two peaks corresponding to DHN and PMB were observed, with a progressive increase in the juglone signal with time. The presence of increasing juglone signal in the reaction mixture was positively identified and characterized by its m/z profile, which also correlated well with its NIST MS signature. This confirmed the feasibility of using DHN juglone as a reliable probe for monitoring rate of SOG, consistent with previous reports regarding its uses as a probe for comparative quantitative analysis [30,31]. However, using GC-MS is not practical for aqueous solutions with macromolecular hosts such as sodium cholate and cyclodextrin, as the organic compounds need to be subject to biphasic extraction, which could result in inaccuracies. Therefore, we deferred studying the SOG rate using UV-Visible spectroscopy as it was direct, and reliable method due to its simplicity and faster reaction times due to low concentration.

A methanolic solution of  $4.92 \times 10^{-5}$  M PMB and  $5.68 \times 10^{-5}$  M DHN was subject to the same experiment involving purging and UV-Vis spectrum recorded every 5 mins. The reaction mixture before exposure to light contained a visible band corresponding to the absorption band in the visible region for PMB and a UV band for the additive absorption of the PMB and DHN chromophores. Upon exposure to light while bubbling oxygen at the rate of 150 mL/min and recording UV-Vis spectrum in a time-dependent manner, changes in the absorption characteristics of the mixture were observed.

The increase in intensity at 240 nm to 280 nm and 350 to 400 nm corresponded to the absorption bands of juglone (Figure 3, left), which are seen around the same region in its pure spectrum; no significant changes in absorption were observed for the PMB visible band. Thus, a plot of increase in absorption intensity around 258 nm and 350 nm with respect to time should represent direct proportionality to the rate of SOG (Figure 4).

We then studied the SOG rate in aqueous medium, wherein an aqueous solution of the same concentration as methanol solution discussed above was prepared from stock solutions as outlined in the experimental section. Due to the low solubility of PMB in water, an immediate dispersion of both compounds was observed in the aqueous medium; DHN did not cause a very high dispersion potentially due to its hydrogen bonding functional groups and higher solubility. The UV-Vis spectrum of

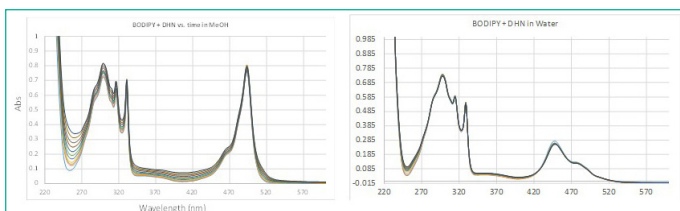


**Figure 3:** (Left) Change in UV-Vis spectrum of solution of PMB ( $4.92 \times 10^{-5}$  M) and DHN ( $5.68 \times 10^{-5}$  M) in methanol purged with oxygen while exposing the solution to white light in 5 mins durations. (Right) Same experiment performed with the compounds dissolved in same concentration in water. Cumulative time of exposure is 0 mins to 50 mins respectively with intervals of 5 mins duration of exposure between each spectrum.

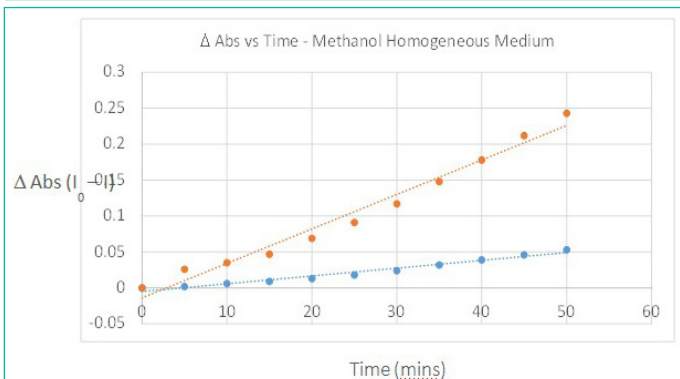


**Figure 4:** Plot showing rate of SO generation as observed through the oxidation of DHN ( $5.68 \times 10^{-5}$  M) with PMB ( $4.92 \times 10^{-5}$  M) experiments outlined in Figure 3. Orange line is change in absorption intensity observed at 258 nm and blue shows the same observed for 350 nm.

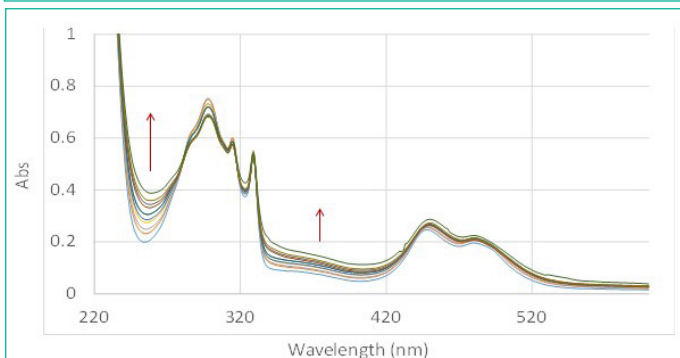


**Figure 5:** Change in UV-Vis spectrum of solution of PMB ( $4.92 \times 10^{-5}$  M) and DHN ( $5.68 \times 10^{-5}$  M) complexed to sodium cholate micelles (11 mM) in water exposed to light under oxygen purging conditions, and recorded in 5 min duration from 0 mins (blue) to 50 mins (green).

the same mixture in predominantly aqueous medium showed some clear differences – low absorption intensity and difference in band ratios, especially for PMB visible region (Figure 3, right). The minimal change in spectra in the time-dependent study and bivariate rate plot (vide infra) clearly showed that no significant SOG occurred. This is attributable to the aggregation induced deactivation of the sensitizer, which is often a major hurdle in the utilization of otherwise efficient sensitizers in PDT.

The SOG efficiency of PMB in aqueous media in presence of sodium cholate at 11 mM concentration was studied at the same concentration of dye and DHN as previously performed experiments (PMB ( $4.92 \times 10^{-5}$  M) and DHN ( $5.68 \times 10^{-5}$  M)) – the reported CMC of sodium cholate is a broad range of 1 to 10 mM determined using various methods [32-35]. Clear change in the UV-Vis spectra showing marked increase in juglone signals indicated that PMB was much more efficient in producing SO (Figure 5). We also performed GC-MS analysis of the reac-

tion mixture performed at higher concentration to confirm the production of oxidized product and its higher prevalence with increasing time. Both the experiments corroborated that sodium cholate was able to solubilize the highly nonpolar sensitizer and enhance its ability to produce singlet oxygen. In terms of the relative SOG rates for PMB in sodium cholate was approximately three-fold as active as that in water without a solubilizer, while it was slightly, but noticeably, lower than that observed in methanol. This was deduced from the time vs. change in absorption max at 258 nm, which is shown in Figure 6. This demonstrates the possibility of using bile salt as drug delivery agent for using non-polar dyes like PMB for PDT.

We then aimed to understand the structure of sodium cholate-solubilized PMB to envision its supramolecular and photo-physical characteristics. For this we calculated energy-optimization of three sodium cholate monomers in aqueous IPCM shell with and without PMB. The IPCM (Integral Equation Formalism Polarizable Continuum Model) is a theoretical framework used in computational chemistry to incorporate the influence of solvents on solute molecules. It treats the solvent as a continuum of varying and uniform dipole for employing integral equations to describe the solute-solvent interactions and allowing for more accurate predictions of molecular properties in the presence of a solvent.

The energy-optimized geometry of three sodium cholate molecules surrounding, and effectively solubilizing, PMB was generated in Spartan '20 at HF STO-3G level of theory (Figure 7). The complex structure showed the nonpolar face of sodium cholate facing inwards with PMB remaining in close contact to the methyl groups. The distance between closest points between four molecules in the aggregate showed a significantly short distance, as shown in Figure 8, indicating an attractive influence, such as van Der Waals interaction holding the aggregate structure together. We also noticed that compared to the initial starting structure the energy optimized aggregate structure had molecular centroids in closer proximity to each other.

Cyclodextrins are macrocyclic hosts that have been used often to disassociate aggregated dyes to reduce non-radiative deactivation to enhance excited state dynamics. Thus, complexing PMB to the  $\beta$ -cyclodextrin ( $\beta$ -CD) was expected to enhance its SOG efficiency by disaggregation, akin to what we observed in sodium cholate. However, to our surprise, photochemical excitation of the dye encapsulated within the macrocycle did not produce any noticeable singlet oxygen (SI Figure 4 and 5). Hence, we employed the larger member of the CD family:  $\gamma$ -CD. Even in this case no noticeable SOG was observed based on the lack of increase in absorbance intensity at 260 nm and 380 nm. Computationally generated complex structure of PMB@  $\gamma$ -CD revealed that the dye fit well within the cavity of the macrocycle (Figure 9) and that the observed reduction in SOG is due to encapsulation. This outcome was not surprising as Sciano *et al* reported the complexation-induced deactivation of SOG efficiency for methylene blue by cucurbituril [36]. Therefore, though CDs have been intuitively expected to facilitate complexation-induced enhancement of excited state dynamics such as energy or electron transfer, in case of PMB dye we did not see such an outcome.

Future studies based on analyzing the emissive and lifetime properties of the complexed molecules to CD and sodium cholate would shed more light into the mechanism of the enhancement and retardation of the BODIPY dyes.

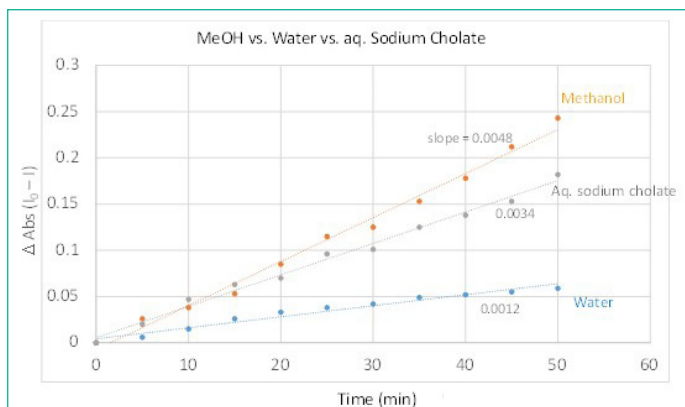


**Figure 6:** Plot showing relative rates of singlet oxygen generation as observed through the oxidation of DHN to produce juglone as the probe reaction in different media and corresponding spectral change at 258 nm: methanol (orange), sodium cholate (gray), and water (blue).

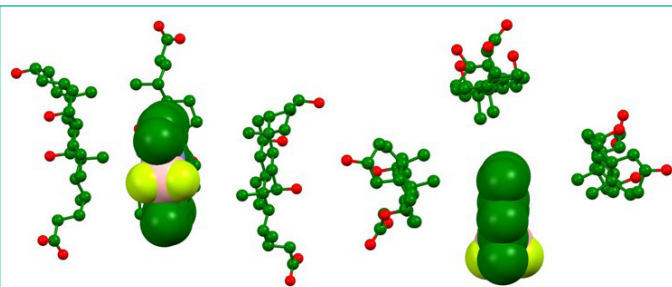


**Figure 7:** Computationally generated representation of bile salt micelle at HF STO-3G in water medium based on IPC model shown from side (left) and top (right). The representation indicates aggregation between three bile salt surfactant sodium cholate (stick and ball model) aggregating around PMB. Hydrogens omitted for clarity.

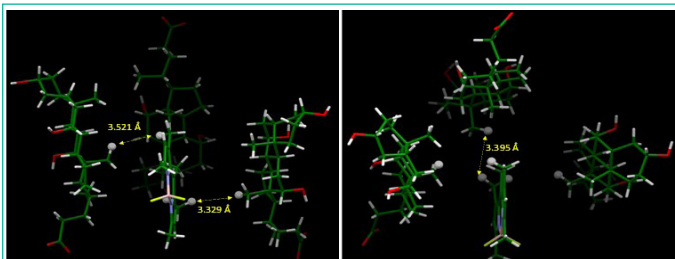


**Figure 8:** Distances between closest points between molecules in the complex based on computationally generated structured (HF STO-3G, water medium IPC model). The close contacts show that the computationally generated aggregate is held-together is sustained by hydrophobic interactions. Hydrogens used for measuring intermolecular distance points are represented in ball model.

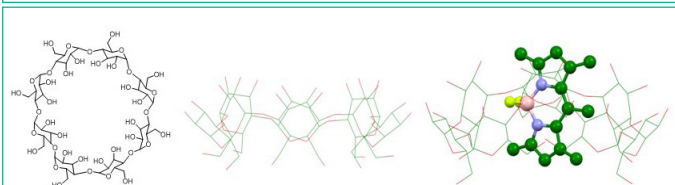


**Figure 9:** Molecular structure (left) and 3D representation (center) of  $\gamma$ -cyclodextrin and its complex (right) with PMB. 3D representations are generated computationally (HF STO-3G, gas phase). Intermolecular distance points are represented in ball model.

## Conclusion

In conclusion, our study highlights the use of bile salt micelles as a supramolecular platform for enhancing the singlet oxygen generation efficiency of a hydrophobic BODIPY dye (PMB) in aqueous media. Our results demonstrate that sodium cholate micelles can solubilize the dye and improve its ability to generate singlet oxygen, while beta-cyclodextrin complex-

ation was found to reduce *SOG*. Computational modeling of the micelle-dye complex structure revealed the presence of attractive intermolecular interactions that contribute to the enhanced photophysical properties. Our findings suggest that bile salt micelles can potentially serve as a safe drug delivery agent for nonpolar dyes like BODIPY in PDT applications. This work not only provides insights into the supramolecular chemistry of bile salt micelles, but also paves the way for the development of more efficient photosensitizers for therapeutic applications.

## Author Statements

## Acknowledgements

MP thanks NU Foundation for purchase of instruments in the UNK campus and his lab.

## Funding

This work is the result of an award from Nebraska Department of Economic Development/Shabri LLC (Contract# 20-01-Funding: 030). The content is solely the responsibility of the authors and does not necessarily represent the official views of the National Institutes of Health.

## Disclaimer/Publisher's Note

The statements, opinions and data contained in all publications are solely those of the individual author(s) and contributor(s) and not of MDPI and/or the editor(s). MDPI and/or the editor(s) disclaim responsibility for any injury to people or property resulting from any ideas, methods, instructions or products referred to in the content.

## References

- Gorman AA, Rodgers MAJ. Singlet molecular oxygen. *Chem Soc Rev.* 1981; 10: 205.
- Ogilby PR. Singlet oxygen: there is indeed something new under the sun. *Chem Soc Rev.* 2010; 39: 3181-209.
- Krieger-Liszky A. Singlet oxygen production in photosynthesis. *J Exp Bot.* 2005; 56: 337-46.
- Hideg E, Kálai T, Hideg K, Vass I. Photoinhibition of photosynthesis in vivo results in singlet oxygen production detection via nitroxide-induced fluorescence quenching in broad bean leaves. *Biochemistry.* 1998; 37: 11405-11.
- Ziegelhoffer EC, Donohue TJ. Bacterial responses to photo-oxidative stress. *Nat Rev Microbiol.* 2009; 7: 856-63.
- Nathan C, Cunningham-Bussel A. Beyond oxidative stress: an immunologist's guide to reactive oxygen species. *Nat Rev Immunol.* 2013; 13: 349-61.
- Dmitrieva VA, Tyutereva EV, Voitsekhovskaja OV. Singlet Oxygen in Plants: Generation, Detection, and Signaling Roles. *Int J Mol Sci.* 2020; 21.
- Di Mascio P, Martinez GR, Miyamoto S, Ronsein GE, Medeiros MHG, Cadet J. Singlet Molecular Oxygen Reactions with Nucleic Acids, Lipids, and Proteins. *Chem Rev.* 2019; 119: 2043-86.
- Frimer AA. The reaction of singlet oxygen with olefins: the question of mechanism. *Chem Rev.* 1979; 79: 359-87.
- Ghogare AA, Greer A. *US Chem Rev (Wash DC).* 2016; 116: 9994-10034.
- Bonnett R. Chemical aspects of photodynamic therapy. *Gordon & Breach.* 2000; 451.

12. Elsaie MLT. Photodynamic therapy: new. Research: Nova Science Publishers, Inc. 2013; 275.
13. Cerro PA, Mascaraque M, Gallego-Rentero M, Almenara-Blasco M, Nicolás-Morala J, Santiago JL et al. Tumor microenvironment in non-melanoma skin cancer resistance to photodynamic therapy. *Front Oncol.* 2022; 12: 970279.
14. de Oliveira AB, Ferrisse TM, Fontana CR, Basso FG, Brighenti FL. Photodynamic therapy for treating infected skin wounds: a systematic review and meta-analysis from randomized clinical trials. *Photodiagn Photodyn Ther.* 2022; 40: 103118.
15. Feng Y, Zeng Q, Qiu Y, Li D, Shi D. Successful application of photodynamic therapy for skin infection caused by *Corynespora casiiicola* in an immunosuppressed patient and literature review. *Photodiagn Photodyn Ther.* 2023; 41: 103279.
16. Foti MC, Amorati R, Baschieri A, Rocco C. Singlet oxygen quenching- and chain-breaking antioxidant-properties of a quercetin dimer able to prevent age-related macular degeneration. *Biophys Chem.* 2018; 243: 17-23.
17. Slutsky-Bank E, Artzi O, Sprecher E, Koren A. A split-face clinical trial of conventional red-light photodynamic therapy versus daylight photodynamic therapy for acne vulgaris. *J Cosmet Dermatol.* 2021; 20: 3924-30.
18. Makuch S, Drozd M, Makarec A, Ziolkowski P, Wozniak M. An Update on Photodynamic Therapy of Psoriasis—Current Strategies and Nanotechnology as a Future Perspective. *Int J Mol Sci.* 2022; 23.
19. Kashyap A, Ramasamy E, Ramalingam V, Pattabiraman M. Supramolecular Control of Singlet Oxygen Generation. *Molecules.* 2021; 26.
20. Naim K, Nair ST, Yadav P, Shanavas A, Neelakandan PP. Supramolecular Confinement within Chitosan Nanocomposites Enhances Singlet Oxygen Generation. *ChemPlusChem.* 2018; 83: 418-22.
21. Liu G, Xu X, Chen Y, Wu X, Wu H, Liu Y. A highly efficient supramolecular photoswitch for singlet oxygen generation in water. *Chem Commun (Camb).* 2016; 52: 7966-9.
22. Carey MC, Small DM. Micelle formation by bile salts. Physical-chemical and thermodynamic considerations. *Arch Intern Med.* 1972; 130: 506-27.
23. Wiedmann TS, Kamel L. Examination of the solubilization of drugs by bile salt micelles. *J Pharm Sci.* 2002; 91: 1743-64.
24. Holm R, Müllertz A, Mu H. Bile salts and their importance for drug absorption. *Int J Pharm.* 2013; 453: 44-55.
25. Nemati M, Fathi-Azarbayjani A, Al-Salami H, Roshani Asl E, Rasmi Y. Bile acid-based advanced drug delivery systems, bilosomes and micelles as novel carriers for therapeutics. *Cell Biochem Funct.* 2022; 40: 623-35.
26. Strauss EW. Electron microscopic study of intestinal fat absorption in vitro from mixed micelles containing linolenic acid, monoolein, and bile salt. *J Lipid Res.* 1966; 7: 307-23.
27. Hofmann AF. The Function of Bile Salts In Fat Absorption. The Solvent Properties of Dilute Micellar Solutions of Conjugated Bile Salts. *Biochem J.* 1963; 89: 57-68.
28. Coello A, Meijide F, Núñez ER, Tato JV. Aggregation behavior of bile salts in aqueous solution. *J Pharm Sci.* 1996; 85: 9-15.
29. Kamkaew A, Lim SH, Lee HB, Kiew LV, Chung LY, Burgess K. BODIPY dyes in photodynamic therapy. *Chem Soc Rev.* 2013; 42: 77-88.
30. Sun J, Zhao J, Guo H, Wu W. Visible-light harvesting iridium complexes as singlet oxygen sensitizers for photooxidation of 1,5-dihydroxynaphthalene. *Chem Commun (Camb).* 2012; 48: 4169-71.
31. Takizawa SY, Aboshi R, Murata S. Photooxidation of 1,5-dihydroxynaphthalene with iridium complexes as singlet oxygen sensitizers. *Photochem Photobiol Sci.* 2011; 10: 895-903.
32. Goheen SC, Matsor RS. *Journal of the American Oil Chemists' Society.* 1989; 66: 994-997.
33. Rinco O, Nolet MC, Ovans R, Bohne C. *Photochemical & Photobiological Sciences.* 2003; 2: 1140-1151.
34. Hebling CM, Thompson LE, Eckenroad KW, Manley GA, Fry RA, et al. Sodium cholate aggregation and chiral recognition of the probe molecule (R,S)-1,1'-binaphthyl-2,2'-diylhydrogenphosphate (BNDHP) observed by <sup>1</sup>H and <sup>31</sup>P NMR spectroscopy. *Langmuir.* 2008; 24: 13866-13874.
35. Singh K, Chauhan S. Temperature dependent micellar behaviour of sodium cholate and sodium deoxycholate in the presence of ceftriaxone sodium: a physicochemical study. *J Mol Liq.* 2020; 316: 113833.
36. González-Béjar M, Montes-Navajas P, García H, Scaiano JC. Methylene blue encapsulation in cucurbit[7]uril: laser flash photolysis and near-IR luminescence studies of the interaction with oxygen. *Langmuir.* 2009; 25: 10490-4.